INVESTIGATION OF AN EXPERIMENTAL EJECTOR COOLING MACHINE OPERATING WITH REFRIGERANT R245fa AND DESIGNED FOR SOLAR AIR CONDITIONING APPLICATIONS

B.J.Huang[1], V.O.Petrenko[1,2] and K.O.Shestopalov[1,2]

[1] New Energy Center, Department of Mechanical Engineering, National Taiwan University, Taipei (Taiwan)

[2] Odessa State Academy of Refrigeration, Ejector Refrigeration Technology Center, Odessa (Ukraine)

bjhuang@seed.net.tw

1. Introduction

Solar cooling technology has been confirmed as a technically viable strategy for suppressing the electrical peak load, because the peak cooling loads are always in phase with the maximum incident solar radiation. The two main components of a solar cooling system are the solar collector and the chiller or air conditioner. The overall efficiency of the system depends on the coupling between these two components.

Ejector cooling machines (ECMs) operating with low boiling point refrigerants are environmentally friendly devices that are suitable for use in solar air conditioning applications due to their simple design and operation, high reliability and durability, and low installation and maintenance costs.

The New Energy Center at National Taiwan University has been devoted to the development of different solar-assisted ejector cooling/heating systems (SACHs) for many years. These SACHs consist of a conventional inverter-type air conditioners (A/C) made of variable-speed compressors connected in series or parallel with solar-driven ECMs. The energy savings of the A/C is experimentally shown to be 50-70% due to the cooling performance of the ECM using R365mfc (Huang et al., 2010a). The long-term performance test results show that the daily energy savings is around 30-70% when compared to the energy consumption of the A/C alone (without solar-driven ECM). The total energy savings of the A/C was 52% over the entire test period (Huang et al., 2010b).

The main objectives of the present research include: (1) to determine a more efficient working fluid for the ECM; (2) to build an ejector test rig for the study of improved ejector construction and ejector flow profile design and performance evaluation; and (3) to design and develop an ECM with an optimal working fluid that will have high coefficients of performance (COPs).

2. Design of solar ejector air conditioners and chillers

A solar ejector air conditioning system consists of a solar collector and a heat driven ECM. The solar collector transforms solar radiation into thermal energy, which then is used to operate the ECM. The main features of a solar ECM are the solar collector and the heating mode of the generator. Figs. 1-3 show the three different methods for heating the generator. Fig. 1 presents a design for a solar ejector air conditioner (SEAC) with direct heating; that is, the surface of the generator is the absorbing plate of the solar collector. Fig. 2 shows a design for a SEAC with a closed-loop mode for circulating a heating medium where heat is supplied by an intermediate heat-transfer liquid – usually water – that is heated in the solar collector. Fig. 3 shows an open-loop mode for heating water that first is used to cool the condenser to reduce the condensing temperature and raise the efficiency of the ejector chiller (Petrenko et al., 2005b).

The process of a continuously operating ECM is characterized by the points 1-9 illustrated in Fig. 4, which shows a diagram of an ejector cooling cycle with the following working principle. Refrigerant is heated and vaporized in the generator by solar thermal energy Q_g at relatively high pressure P_g. This motive vapor, with a mass flow rate $\dot{m}_p$, flows through the primary nozzle of the ejector. At the exit of the nozzle, the accelerated flow becomes supersonic, which produces a low-pressure region in the suction chamber of the ejector.

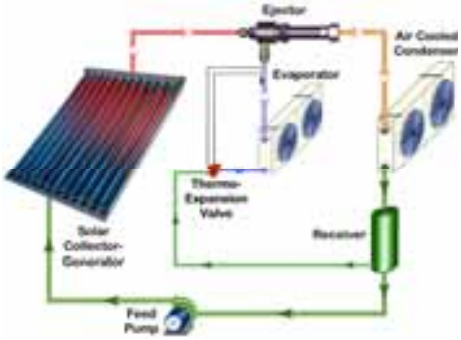

Fig. 1: Design of a solar ejector air conditioner with direct heating

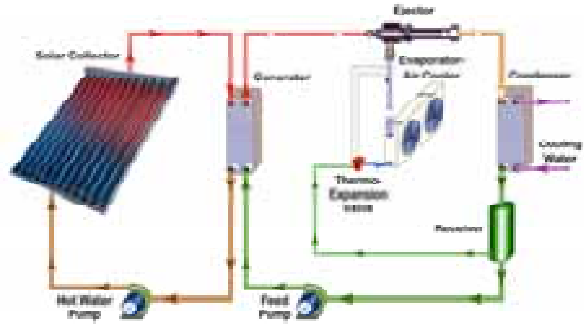

Fig. 2: Design of a solar ejector air conditioner with a closed-loop mode for circulating heating medium

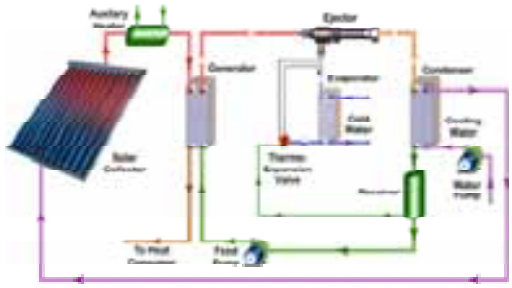

Fig. 3: Design of a solar ejector chiller with an open-loop mode for the heating medium

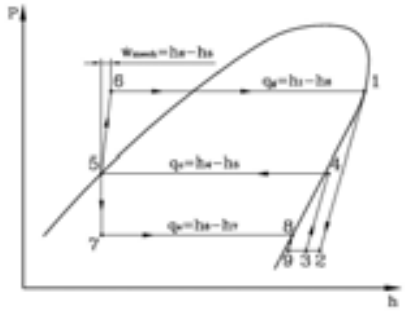

Fig. 4: Diagram of thermodynamic cycle of ECM

Hence, vapor, at low pressure P_e, with a flow rate of $\dot{m}_s$, is induced from the evaporator into the ejector. Primary and secondary fluids are mixed in the mixing section of the ejector and these then undergo a pressure recovery process in the diffuser section. The combined stream flows to the condenser where it is condensed into liquid at intermediate pressure P_c. The heat of condensation Q_c is rejected to the environment. Some of the condensate is returned to the solar-powered generator via an electrically driven feed pump, consuming mechanical power $\dot{W}_{mech}$, whilst the remainder expands as it flows through a valve before returning to the evaporator, where it re-evaporates to produce the necessary cooling effect Q_e.

3. Analysis of ejector design and ejector cooling cycle performance

The supersonic ejector is the key component in the ejector refrigeration cycle. It is a simple jet device which is used in the ejector cycle for suction, compression and discharge of the secondary vapor by the force of the primary vapor.

Fig. 5 illustrates the structure of the advanced supersonic ejector with two symmetrical suction inlets inclined to the axis of the ejector. The ejector consists of four main parts: a supersonic nozzle, a suction chamber, a cylindrical mixing chamber and a diffuser. The design of the ejector with two retrofract symmetrical suction inlet ducts provides both axisymmetric equal distribution of the secondary flow in the suction chamber and a significant decrease in shock losses, which occur in the suction and mixing chambers of the ejector.

Operating conditions of an ejector are specified by the operating pressures P_e, P_c, P_g, the expansion pressure ratio $E = P_g/P_e$ and the compression pressure ratio $C = P_c/P_e$.

The performance of an ejector is measured by its entrainment ratio ω, which is defined as:

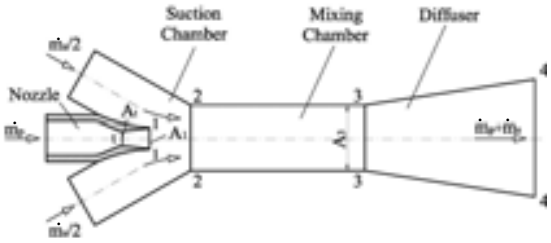

Fig. 5: Structure of the advanced ejector

$$\omega = \frac{\dot{m}_s}{\dot{m}_p} \quad \text{(eq. 1)}$$

Construction, geometry and surface condition of the supersonic ejector flow profile must provide the most effective utilization of primary flow energy for suction, compression and discharge of the secondary vapor (Huang et al., 2001; Petrenko, 1978; Petrenko, 2001; Petrenko et al., 2005b).

The performance of the ECM is usually measured by a single coefficient of performance (COP), which is the ratio of the useful cooling effect Q_e produced in the condenser over the gross energy input into the ejector cycle. However, the fact that the ECM commonly utilizes a mechanical feed pump should be taken into account, and, consequently, it requires an input of some amount of mechanical power $\dot{W}_{mech}$ in addition to a low-grade heat energy Q_g.

The mechanical power $\dot{W}_{mech}$, consumed by the feed pump is very small compared to the thermal energy Q_g input to the generator to actuate ejector cycle, but it may not be neglected (Petrenko, 2001). Therefore, from both thermodynamic and economic points of view, the efficiency of the ECM cycle can be correctly characterized by separate use of both the thermal COP_{therm} and the actual specific power consumption of mechanical feed pump $\dot{w}_{mech}$, which are defined respectively as:

$$COP_{therm} = \frac{Q_e}{Q_g} = \frac{\dot{m}_s q_e}{\dot{m}_p q_g} = \omega \frac{q_e}{q_g} \quad \text{(eq. 2)}$$

$$\dot{w}_{mech} = \frac{\dot{W}_{mech}}{Q_e} = \frac{\dot{m}_p v_5 \left(P_g - P_c\right)}{\eta_{pump}\, \dot{m}_s q_e} = \frac{v_5 \left(P_g - P_c\right)}{\eta_{pump} \omega\, q_e} \quad \text{(eq. 3)}$$

where v_5 and η_{pump} are the specific volume of intake refrigerant and feed pump coefficient of efficiency, respectively and $(P_g - P_c)$ is the generating and condensing pressure difference, in kPa.

Analysis of Eqs. (eq. 2) and (eq. 3) shows that COP_{therm} and $\dot{w}_{mech}$ strongly depend on the operating conditions, the efficiency of the ejector and the thermodynamic properties of the refrigerant used.

Clearly, reliable performance of the ECM depends very much on the reliability of feed pump operation, which is the critical component in the ejector cycle. This electrically actuated pump is the only element in the heat-driven ECM that has moving parts and therefore it determines the reliability, leak resistance and lifetime of the whole system.

The reliable operation of the feed pump is largely determined by the pressure difference (P_g-P_c). The best way to decrease this pressure difference, and thereby to increase the dependability of the system as a whole, is to use low-pressure refrigerants in the ejector refrigeration cycle.

4. Refrigerant selection and simulation of the ejector cooling cycle performance

The analysis and comparison of performance characteristics of various refrigerants showed that, from thermodynamic and operating viewpoints, the most suitable refrigerants for ECMs are low-pressure types with high critical temperature T_{cr}, large specific latent heat of vaporization at temperatures T_e and T_g, small specific heat of liquid refrigerant in the range of operating temperatures (T_g-T_e) and a normal boiling point temperature T_b about T_e (Petrenko, 2001; Petrenko et al., 2005a).

Fig. 6 shows saturation curves of different low-pressure refrigerants in a *T-s* diagram and Table 1 presents several parameters of these working fluids for comparison, to allow selection of the most appropriate one. The analysis and comparison of performance characteristics of these refrigerants confirms that the

environmentally friendly low-pressure hydrocarbons R600, R600a and working fluid R245fa offer the best performance combinations and, at present, are the most suitable choices for application in ejector chillers and air conditioners.

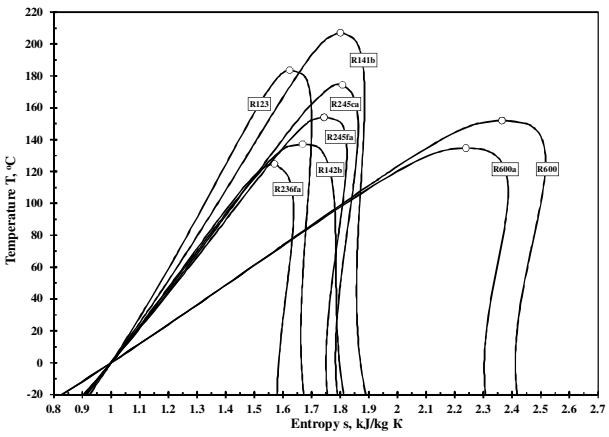

Fig. 6: Saturation curves of different low-pressure refrigerants in T-s diagram

Hydrocarbons are well-known gases and can be found in a number of general applications. Their use in systems for commercial refrigeration, chillers and heat pumps is well established (Granryd, 2001). Results of investigations of ECMs operating with various hydrocarbon refrigerants have also been reported in recent years (Selvaraju and Mani, 2004; Pridasawas and Lundqvist, 2007; Nehdi et al., 2008; Boumaraf and Lallemand, 2009; Raul Roman and Hernandez, 2009). A number of hydrocarbons have favorable characteristics as refrigerants from a thermodynamic, as well as a heat transfer, point of view. They have excellent environmental characteristics: no Ozone Depleting Potential and negligible Global Warming Potential. Hydrocarbons have been utilized as refrigerants for many years in the petrochemical industry. Experience gained in recent years indicates that the use of hydrocarbons can be implemented in an economical way for a number of other applications. However, safety precautions due to their flammability must be seriously taken into account (Granryd, 2001).

Refrigerant R245fa also has good thermodynamic properties, reasonable working pressures and a high critical temperature that makes it a useful candidate fluid for an ejector cooling cycle. In addition, it is non-corrosive, non-toxic and non-flammable. For these reasons, refrigerant R245fa is selected as the most suitable working fluid for general purpose applications in the present study (Petrenko et al., 2005a).

Tab. 1: Table of properties for different low-pressure refrigerants

Property \ Refrigerant	R123	R141b	R142b	R236fa	R245ca	R245fa	R600	R600a
Chemical Formula	$C_2F_3HCl_2$	$C_2FH_3Cl_2$	$C_2H_3F_2Cl$	$C_3H_2F_6$	$C_3H_3F_5$	$CHF_2CH_2CF_3$	C_4H_{10}	C_4H_{10}
Molecular Weight M, kg/kmol	152.93	116.9	100.5	152.04	134.05	134.05	58.13	58.13
Normal Boiling Temperature T_b, °C	27.87	32.20	-9.80	-1.44	25.13	14.90	-0.50	-11.61
Critical Temperature T_{CRIT}, °C	183.8	208.0	137.4	124.92	174.4	154.05	152.0	134.7
Critical Pressure P_{CRIT}, bar	36.7	43.4	42.0	32.0	39.3	36.4	37.9	36.4
Specific Heat Capacity of Liquid c_p at T = 30°C, kJ/kg	1.025	1.15	1.19	1.28	1.34	1.37	2.47	2.49
Latent Heat h_{fg} at T = 8°C, kJ/kg	178.3	234.0	209.4	155.4	210.0	200.6	377.9	347.8
Ozone Depletion Potential (ODP)	0.02	0.11	0.06	0.00	0.00	0.00	0.00	0.00
Global Warming Potential (GWP)	90	630	2000	9400	950	950	0.00	0.00
Flammability	No	Yes	Yes	No	No	No	Yes	Yes

The ejector and ECM performance were determined using a computer simulation program based on the 1-D theory of the ejector. This program predicts the performance and geometry of the ejector at critical-mode operating conditions and provides optimum design data for the ejector and ECM (Huang et al., 1999; Petrenko et al., 2005a). The model validation against the experimental data obtained for refrigerants R141b, R236fa and R245fa has shown very good agreement under a wide range of operating conditions (Huang et al., 1999; Eames et al., 2004; Eames et al., 2007).

This program was used for theoretical study of a supersonic ejector with a constant-area mixing chamber operating with R245fa. The ejector and ECM were studied over the range of critical condensing temperatures $T_c = 30 - 40$°C, and operating generating temperatures T_g of 90, 95 and 100°C at the evaporating temperatures $T_e = 8$, 12 and 16°C. All calculations were performed using REFPROP 8.0 (Lemmon et al., 2007).

Figs. 7-12 illustrate the variations in the theoretical ω, COP_{therm} and A_3/A_t with T_c at different T_g and $T_e = 8$, 12 and 16°C. Figs. 7, 9 and 11 show that the characteristic ω and COP_{therm} have the same trend: they increase with decreasing T_c and increasing T_g. Figs. 8, 10 and 12 show that the area ratio A_3/A_t decreases with increasing T_c and decreasing T_g.

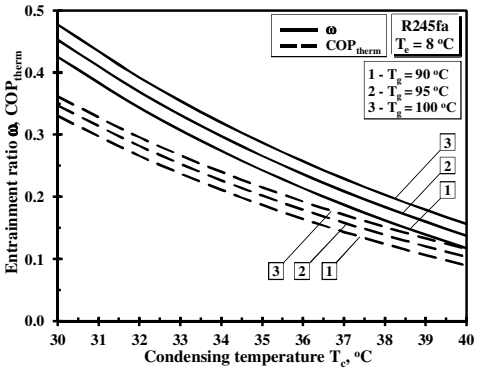

Fig. 7: Variation in ω and COP_{therm} with T_c at different T_g and $T_e = 8^o$C

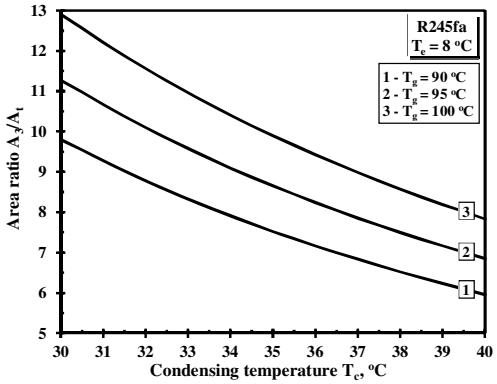

Fig. 8: Variation in A_3/A_t with T_c at different T_g and $T_e = 8^o$C

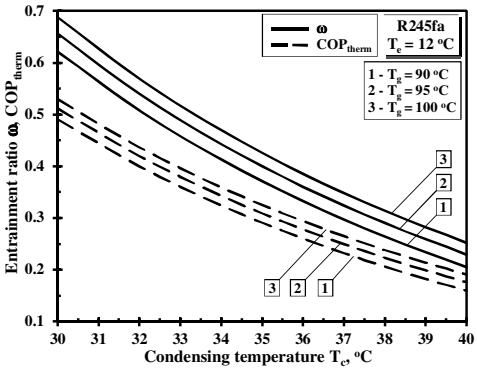

Fig. 9: Variation in ω and COP_{therm} with T_c at different T_g and $T_e = 12^o$C

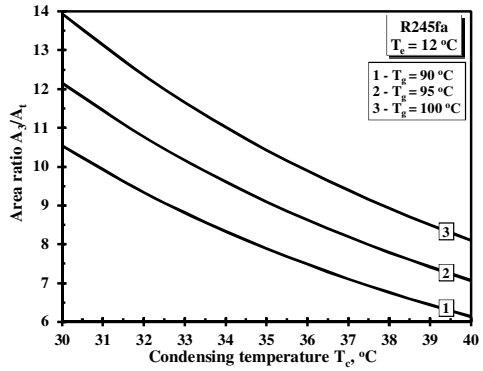

Fig. 10: Variation in A_3/A_t with T_c at different T_g and $T_e = 12^o$C

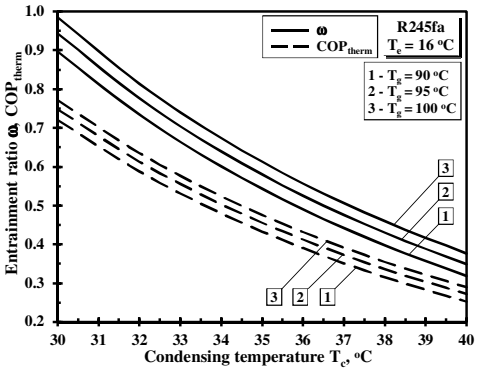

Fig. 11: Variation in ω and COP_{therm} with T_c at different T_g and T_e = 16°C

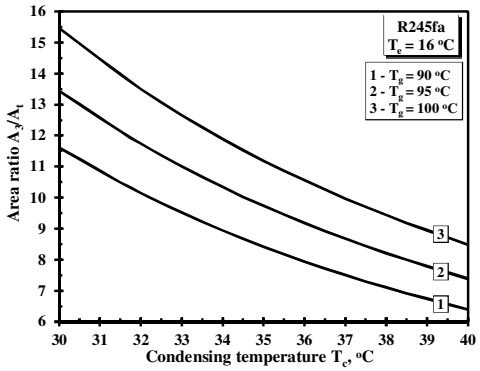

Fig. 12: Variation in A_3/A_t with T_c at different T_g and T_e = 16°C

5. Description of the experimental setup

To verify the theoretical analysis of the ejector geometry and performance characteristics of the ECM using refrigerant R245fa, an ejector test rig with a cooling capacity of 10.5kW (3RT) was designed and constructed. A schematic diagram and a photograph of the ejector test rig are shown in Figs. 13 and 14, respectively. The ejector test rig equipment includes the following nine major components: an experimental ejector, a generator, an evaporator, a condenser, a receiver-subcooler, a float regulating valve, a gear-type feed pump, a cooling tower and a control panel equipped with different measurement instrumentation. Locations of measurement points around the circuit are shown in Fig. 13.

A photograph of the experimental ejector assembly with two retrofract symmetrical suction inlet ducts and a suction manifold is shown in Fig. 15. The assembly of the ejector consists of the following main components: a body, an axially movable supersonic nozzle, a mixing chamber made jointly with the diffuser, a frame and a mechanism to move the nozzle into optimal position with respect to the entrance of the mixing chamber. The ejector assembly is 510 mm in length, 60 mm in height and 130 mm in width. Photographs of the tested supersonic nozzle and cylindrical mixing chamber made jointly with the diffuser are shown in Fig. 16 and Fig. 17, respectively; their specifications are listed in Table 2.

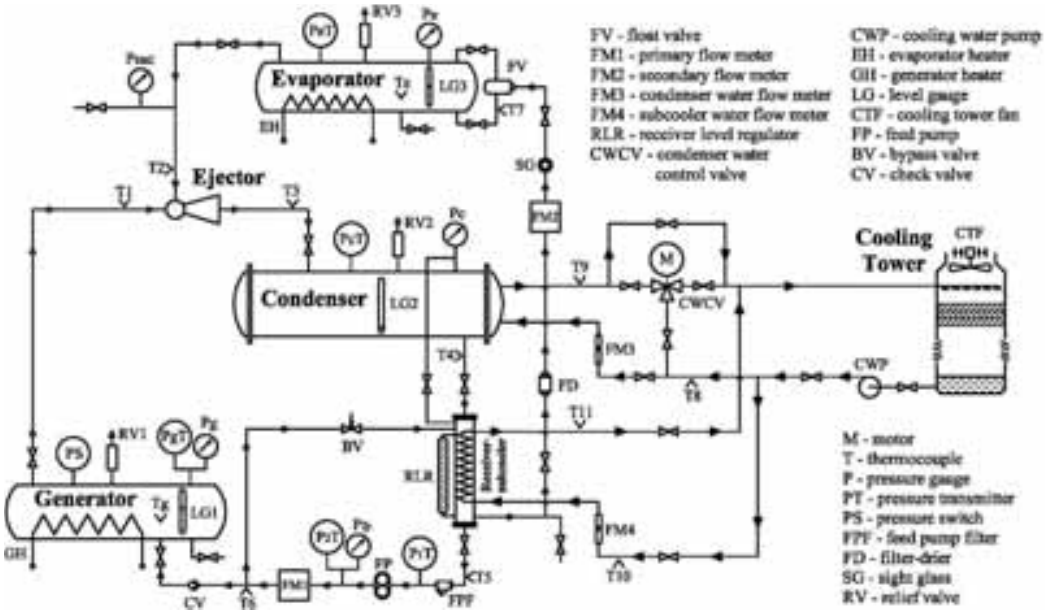

Fig. 13: Schematic diagram of the ejector test rig

Fig. 14: Photograph of the ejector test rig

Fig. 15: Photograph of the ejector assembly

Fig. 16: Photograph of the tested supersonic nozzle

Fig. 17: Photograph of the tested mixing chamber

Tab. 2: Specification of the supersonic nozzle and constant-area mixing chamber

Primary nozzle design		**Constant-area mixing chamber design**	
Throat diameter, d_t	4.212 mm	Constant area section diameter, d_3	13.02 mm
Throat area, A_t	13.93 mm^2	Constant section area, A_3	133.07 mm^2
Exit diameter, d_1	7.11 mm	Length of constant area section, l_{mch}	98.64 mm
Exit area, A_1	39.68 mm^2	Length of diffuser, l_d	135.75 mm
Area ratio, A_1/A_t	2.85	Diverging angle of diffuser	8.0˚
Convergent angle of nozzle	30˚	Exit diameter of diffuser, d_4	32.0 mm
Diverging angle at nozzle exit	6.0˚	Exit area of diffuser, A_4	803.84 mm^2

The generator was designed with a cylindrical shape and had a glass level gauge for liquid level observation. The working fluid in the generator was heated by two 13kW electric heaters that were separately controlled, as were the heat load, generating temperature and pressure. The evaporator was also designed in a cylinder shape with a glass level gauge for liquid level observation. Heat energy was directly transferred to the evaporator by two 6 kW electric heaters to simulate the evaporator cooling load. The electric heaters were also separately controlled, as were the cooling load, evaporating temperature and pressure. Electric energy inputs to the generator and evaporator were measured by electrical power meters. The generator and evaporator and all of their connecting lines were thoroughly thermally insulated. The condenser was a conventional shell-and-tube heat exchanger with a glass level gauge, cooled by water supplied from the cooling tower, with a rejected heat capacity of 52 kW. The condenser temperature and the ejector backpressure were automatically controlled by varying the water flow through the condenser. The receiver-subcooler was a specially designed shell-and-coil type vertical vessel cooled by water taken from the cooling tower. It was equipped with a level gauge and level transmitter for liquid level observation and control. The receiver-subcooler and all of its connecting lines were thermally insulated. A hydraulic gear-type pump driven by a three-phased variable speed electric motor was used as the generator feed pump. Primary and secondary flow rates were measured by gear-type flow meters. The pressures of the primary and secondary flows, the back pressure at the condenser and the pressure after feed pump were measured using industrial direct-reading pressure gauges and pressure transmitters. Suction and condensing pressures were measured using high-precision Bourdon-tube gauges. Several K-type thermocouples were installed at appropriate

places (T_1-T_{11}) for temperature measurement. RTD sensors were used to control the generating, evaporating and condensing temperatures. The generator, evaporator and condenser were protected by pressure relief valves. The flow rates of the cooling water circulating through the condenser and receiver-subcooler were measured by glass flow meters. A control panel equipped with different instrumentation and other various standard components of the refrigeration machine were also used in the construction of the ejector test rig. Specifications of the main measurement instrumentation of the ejector test rig are given in Table 3.

A PC-based monitoring and control system was developed in the present study for the ejector test rig. The data were sampled by a data acquisition system every 10 seconds. Pressures, temperatures, primary and secondary flow rates, electric power consumption and other required data were recorded and the results were calculated. This enabled the main performance to be determined in a steady state condition of system operation.

Tab. 3: Specifications of the measurement instrumentation of the ejector test rig

Parameters	Instruments	Ranges	Accuracy
Temperature T_g	RTD sensor	0~200ºC	±0.12%
Temperatures T_e, T_c	RTD sensors	0~50ºC	±0.12%
Temperatures T_1-T_{11}	K-type thermocouples	-200~320ºC	±1.5ºC
Pressures P_g, P_e, P_c, P_{fp}	Industrial pressure gauges	-1~30 bar	±1.5%
Pressure P_{suc}	Bourdon-tube pressure gauge	-1~1 bar	±0.25%
Pressure P_c	Bourdon-tube pressure gauge	-1~2 bar	±0.25%
Refrigerant flow rates	Gear-type flow meters	0.1~6.0 l/min	±3.0%
Electric energy input	Electrical power meters	0~30 kW	±0.6%

6. Experimental results and discussion

The first task of the experiments that used R245fa was to calibrate the supersonic nozzle under different generating temperatures and pressures. In these tests, the rig was run with a closed suction line. The calibration test for the nozzle was repeated 4 – 6 times to ensure that no variation occurred with the data taken from the generator heaters. The primary flow was determined from the energy balance of the generator and it was also measured using a flow meter. The theoretical mass flow rate through the nozzle can be expressed by:

$$\dot{m}_p = A_t \cdot P_g \frac{k}{\sqrt{\frac{2 \cdot k}{k+1} \cdot \frac{P_g}{\rho_1}}} \cdot \left(\frac{2}{k+1}\right)^{\frac{k}{k-1}} \cdot \mu \qquad \text{(eq. 4)}$$

where k is heat capacity ratio, μ - flow coefficient.

Fig. 18 shows the comparison of the measured mass flow rate and calculated values for a nozzle with d_t = 4.212 mm. The calculated values with flow coefficient $\mu = 0.95$ agree very well with the measured data. Therefore the subsequent experimental data were converted using calculated primary mass flow rates instead of the measured ones.

Once the supersonic nozzle was calibrated over a range of generating temperatures, the cooling machine was ready to conduct the full test for the designed ejector geometry over a range of design and off-design operating conditions.

For each test run, the generator heaters were switched on and set to the desired heat load input. When the designed temperature in the generator was reached, the control valves on secondary flow line and on the primary flow line were opened, and at the same time the feed pump and evaporator heaters were switched on. The pressures at the generator and evaporator were controlled by adjusting the power consumption of the appropriate electric heaters. By circulating cooling water from the cooling tower the condensing pressure was maintained at the desired value using a 3-way control valve. The flow of cooling water through the

receiver-subcooler was adjusted by an appropriate shutoff water valve and the cooling water flow was varied during the tests, depending on the operating conditions.

The experimentation was carried out by varying the temperatures individually in the evaporator, condenser and generator. For each test the critical condensing temperature was established and determined.

Some of the test results obtained for the ejector cycle are shown in Figs. 19 – 21. These data were obtained with an ejector with an area ratio A_3/A_t=9.55 and optimal position of the nozzle l_n=21mm in the front of the entry section of the cylindrical mixing chamber. An ejector using R245fa was designed for operation at T_g = 95˚C and T_e = 12˚C. Figs. 19 – 21 show the effect of the condensing temperature T_c on the ejector and ECM performance for evaporating temperatures T_e varying from 8 to 16˚C and T_g = 95˚C. For each given T_e, the entrainment ratio ω, thermal coefficient of performance COP_{therm} and cooling capacity Q_e are independent of the ejector back pressure, i.e. the condensing temperature and pressure. However, when the condensing temperature T_c is higher than a certain value, known as the "critical condensing temperature" T_c^*, then ω, COP_{therm} and Q_e will decrease suddenly and then fall to zero (Huang et al., 1985).

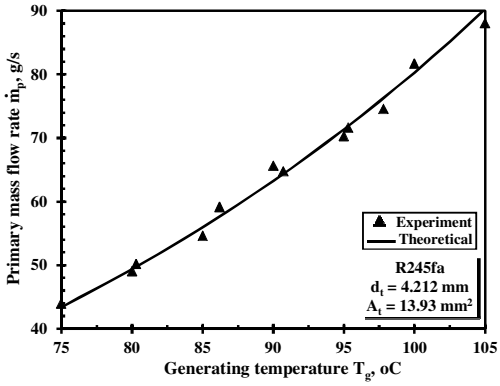

Fig. 18: Comparison of the measured and calculated primary mass flow rate values for nozzle with d_t = 4.212 mm

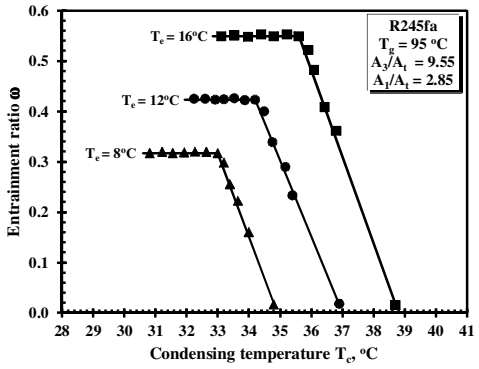

Fig. 19: Measured variation in ω with T_c at different T_e

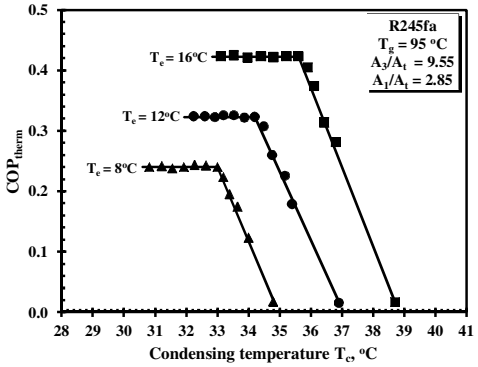

Fig. 20: Measured variation in COP_{therm} with T_c at different T_e

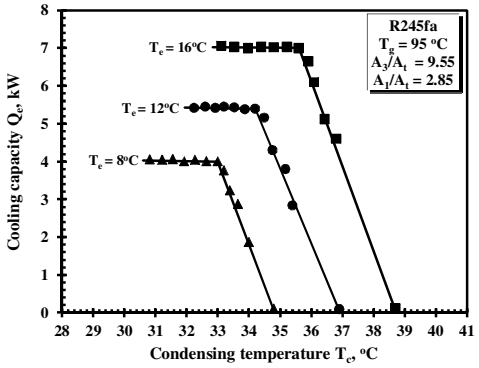

Fig. 21: Measured variation in Q_e with T_c at different T_e

From obtained experimental results, it follows that the critical condensing temperature varies with generating and evaporating temperatures. This is therefore an important design criterion, which is determined by the highest temperature anticipated at the condenser heat sink. The optimum ejector and ECM performances can be obtained when the system operates at critical condensing temperatures. At a constant generating temperature, higher values of ω, COP_{therm} and Q_e can be achieved when the evaporating temperature is allowed to rise. Therefore, for air conditioning applications, it is preferable to design an ejector for high evaporating temperatures. This then leads the ECM to operate at higher critical condensing temperatures as the condenser heat sink temperature increases.

In practice, the actual operating temperatures T_c, T_g and T_e vary with the surrounding conditions and usually are adjustable. A method for the determination of the optimal adjustment range subject to the requirements of the refrigeration user and concrete application conditions is given in Petrenko and Volovyk (2007). This method enables one to select the combination of three independent operating parameters T_e, T_c and T_g to provide maximum efficiency of the ECM at double critical off-design operating conditions.

The theoretical and experimental results were used to construct performance maps. Figs. 22 – 24 show the theoretical (dotted lines) and measured (solid lines) variations in ω, $\mathrm{COP}_{\mathrm{therm}}$ and Q_e with the critical condensing temperatures over a range of evaporating and generating temperatures.

From Figs. 22 – 24, for experimental data, it follows that at the given adjustment range of T_e, which varied from 8 to 16 ºC, in order to achieve the maximum performance of ECM with a variation of T_c in the range of 29.6 – 39.0 ºC, the temperature T_g must also be adjusted in the range of 88.0 – 102.0 ºC. Under these conditions, the characteristics ω, $\mathrm{COP}_{\mathrm{therm}}$ and Q_e will take on various intermediate values in the following ranges: $\omega = 0.23 - 0.70$, $\mathrm{COP}_{\mathrm{therm}} = 0.17 - 0.55$ and $Q_e = 3.3 - 7.8$ kW.

Theoretical data show good coincidence with experimental results not only for the design point (T_g=95ºC, T_e=12ºC), but also for other off-design points. The maximum difference between the experimental results and the results of the proposed model is about 5%.

The ECM performance maps provide useful assistance for the development of an automatic control system for the ECM operating at off-design double critical operating conditions. Obtained test results demonstrate that solar energy or low-grade heat can be used to drive efficient ECMs operating with R245fa for air conditioning and space cooling.

Extensive data for the feed pump operation were obtained. Fig. 25 shows how the measured feed pump capacity increased with generating pressure P_g at constant $P_c = 2.12$ bar and $T_c = 35$ ºC. Considering the important function of the circulating feed pump in the system, other main pump characteristics have been investigated including feed pump motor speed n and feed pump power consumption W_{fp}. From Figs. 26-27 it follows that measured motor speed n, as well as theoretical power consumption W_{fp} increase with increases in the feed pump pressure difference (P_g-P_c). This trend is not unexpected because if the generating temperature and pressure of refrigerant are rising at invariable T_c and P_c, this will result in increased power consumption to pump this refrigerant.

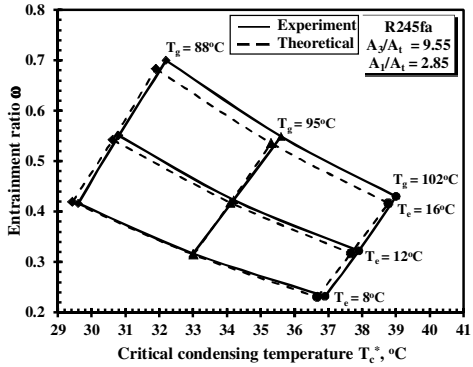

Fig. 22: Measured and theoretical variation in ω with T_c* over a range of T_e and T_g

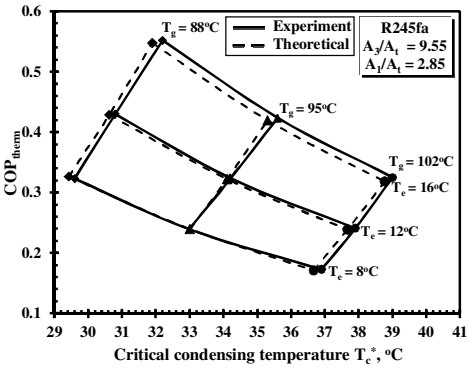

Fig. 23: Measured and theoretical variation in $\mathrm{COP}_{\mathrm{therm}}$ with T_c* over a range of T_e and T_g

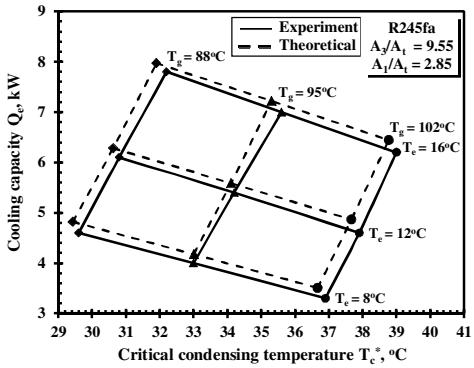

Fig. 24: Measured and theoretical variation in Q_e with T_c* over a range of T_e and T_g

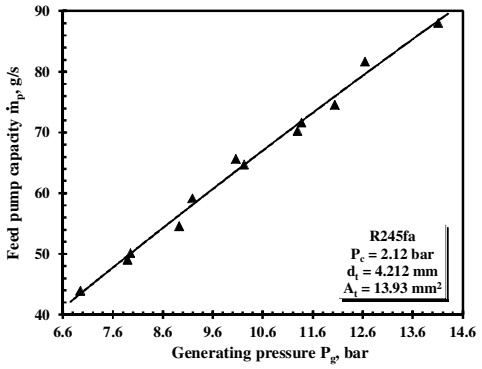

Fig. 25: Variation in feed pump capacity $\dot{m}_p$ with generating pressure P_g

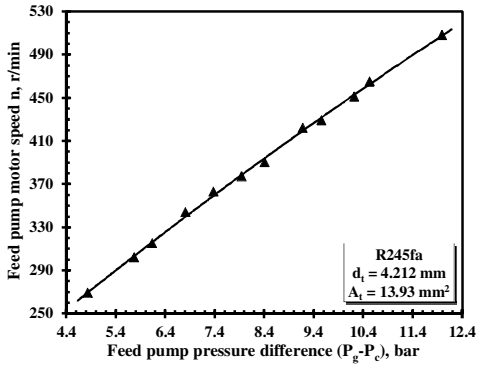

Fig. 26: Variation in feed pump motor speed with pressure difference (P_g-P_c)

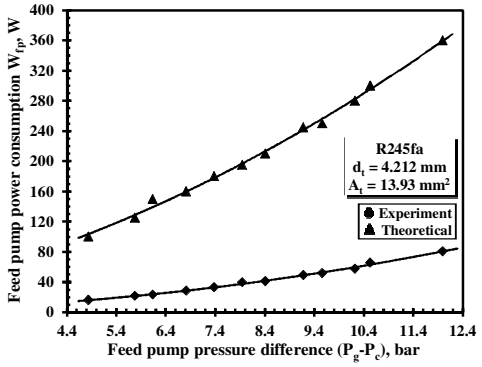

Fig. 27: Variation in experimental and theoretical feed pump power consumption with pressure difference (P_g-P_c)

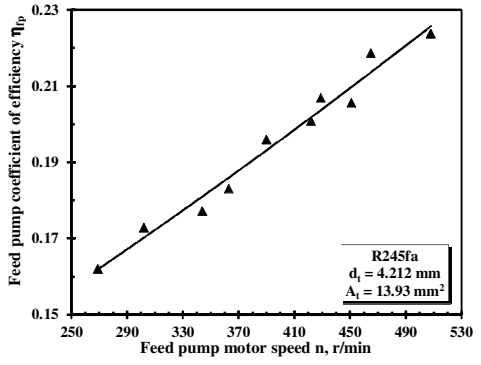

Fig. 28: Variation in experimental feed pump coefficient of efficiency η_{fp} with feed pump motor speed n

Fig. 28 shows that the experimental feed pump coefficient of efficiency η_{fp} increases with increases in the feed pump motor speed n.

Analysis of the obtained results shows that the feed pump electrical power consumption at design and near design operating conditions is about 0.24-0.26 kW, which is not higher than 1.6% of the generating heat load Q_g. At this condition, the actual specific power consumption of feed pump w_{mech} reaches a value of 0.05 kW kW^{-1}.

7. Conclusions

This paper presents the results of a theoretical and experimental investigation of an ejector and ejector cooling machine designed for a solar air conditioning application. The main findings of the present study can be summarized as follows:

- On the basis of the analysis and comparison of performance characteristics for various refrigerants, the environmentally friendly working fluid R245fa is selected for the present study because it offers the best performance combinations for application in ejector chillers and air conditioners.
- The effect of the ejector cycle operating conditions on the ejector and ECM performance characteristics is studied; experimental results are in good agreement with the theoretical data.
- The obtained test results demonstrate that low-grade heat from solar collectors can be used to drive efficient ECMs operating with R245fa and designed for air conditioning and space cooling.

Acknowledgment

This publication is based on the work supported by Award No.KUK-C1-014-12, made by King Abdullah University of Science and Technology (KAUST), Saudi Arabia.

8. References

Boumaraf, L., Lallemand, A., 2009. Modeling of an ejector refrigerating system operating in dimensioning and off-dimensioning conditions with the working fluids R142b and R600a. Applied Thermal Engineering 29, 265-274.

Eames, I.W., Ablwaifa, A.E., Petrenko, V.O., 2007. Results of an experimental study of an advanced jet-pump refrigerator operating with R245fa. Applied Thermal Engineering 27, 2833-2840.

Eames, I.W., Petrenko, V.O., Ablwaifa, A.E., 2004. Design and experimental investigation of a jet pump refrigerator. 3rd International Conference on Heat Powered Cycles – HPC Larnaca, Cyprus.

Granryd, E., 2001. Hydrocarbons as refrigerants - an overview. International J. of Refrigeration 24, 15-24.

Huang, B.J., Chang, J.M., Wang, C.P., Petrenko, V.O., 1999. A 1-D analysis of ejector performance. International Journal of Refrigeration 22(5), 354-364.

Huang, B.J., Jiang, C.B., Fu, F.L., 1985. Ejector performance characteristics and design analysis of jet refrigeration system. ASME J. Engng Gas Turbines and Power 107, 792–802.

Huang, B.J., Petrenko, V.O., Samofatov, I.Y., Shchetinina, N.A., 2001. Collector selection for solar ejector cooling systems. Solar Energy 71, 269-274.

Huang, B.J., Wu, J.H., Hsu, H.Y., Wang, J.H., 2010a. Development of Hybrid Solar-assisted Cooling/Heating System. Energy Conversion and Management 51, 1643–1650.

Huang, B.J., Yeh, C.W., Wu, J.H., Liu, J.H., Hsu, H.Y., Petrenko, V.O., Chang, J.M., Lu, C.W., 2010b. Optimal control and performance test of solar-assisted cooling system. Applied Thermal Engineering 30, 2243-2252.

Lemmon, E.W., Huber, M.L., McLinden, M.O., 2007. NIST Standard Reference Database 23: Reference Fluid Thermodynamic and Transport Properties-REFPROP, Version 8.0. Gaithersburg.

Nehdi, E., Kairouani, L., Elakhdar, M., 2008. A solar ejector air conditioning system using environment-friendly working fluids. Int. J. Energ. Res. 32, 1194-1201.

Petrenko, V.O., 1978. Investigation of ejector cooling machine operating with refrigerant R142b. Ph.D. thesis. Odessa Technological Institute of Refrigeration Industry, Ukraine.

Petrenko, V.O., 2001. Principle of working fluid selection for ejector refrigeration systems. Refrigeration Engineering and Technology 1 (70), 16-21.

Petrenko, V.O., Chumak, I.G., Volovyk, O.S., 2005a. Comparative analysis of the performance characteristics of an ejector refrigerating machine utilizing various low-boiling working fluids. Refrigeration Engineering and Technology 5 (97), 25-35.

Petrenko, V.O., Volovyk, O.S., 2007. Analysis of performance characteristics of ejector refrigeration machine operating at design and off-design conditions. Refrigeration Engineering and Technology 2(106), 20-26.

Petrenko, V.O., Volovyk, O.S., Ierin, V.O., 2005b. Areas of effective application of ejector refrigeration machines using low-boiling refrigerants. Refrigeration Engineering and Technology 1, 17-30.

Pridasawas, W., Lundqvist, P., 2007. A year-round dynamic simulation of solar-driven ejector refrigeration system with iso-butane as a refrigerant. International Journal of Refrigeration 30, 840-850.

Raul Roman, A., Hernandez, J., 2009. Performance of ejector cooling systems using hydrocarbon refrigerants. EUROTHERM SEMINAR №85, Louvain-la-Neuve, Belgium.

Selvaraju, A., Mani, A., 2004. Analysis of an ejector with environment friendly refrigerants. Applied Thermal Engineering 24, 827-838.